

Research Article

In silico drug discovery of flavonoids as potential PPAR agonists in treatment of metabolic syndrome

Bao Hoang Gia Nguyen, Phuong Chau Uyen Nguyen, Khoi Anh Nguyen, Phat Nguyen Pham, Phuong Thuy Viet Nguyen*

Faculty of Pharmacy, University of Medicine and Pharmacy at Ho Chi Minh City, Ho Chi Minh City, Viet Nam

ABSTRACT

Peroxisome proliferative activating receptors (PPARs) are a subfamily of three ligand-inducible transcription factors which are important targets in drug discovery for the treatment of metabolic syndrome (MetS). This study aimed to discover flavonoids as potential PPAR agonists. The results showed that the generated 3D-pharmacophore model for PPAR activators included four pharmacophoric features, namely one hydrophobic, two hydrogen acceptors and one hydrogen donor points, respectively. This pharmacophore model had the specificity, accuracy and sensitivity were 74%, 74% and 75%, respectively. 648 out of 3,848 flavonoid compounds satisfied all the features of the chosen pharmacophore model. Molecular docking results demonstrated that these compounds bound well in the binding site of PPARs. Among them, F85 was the most potential compound with the binding affinities of PPAR α (-9.6 kcal.mol⁻¹), PPAR γ (-10.5 kcal.mol⁻¹), PPAR δ (-9.5 kcal.mol⁻¹). Through forming hydrogen bonds and hydrophobic interactions with the key residues, F85 could reach deeper into the binding pocket of the receptors. Moreover, F85 was stable in the binding site of PPARs during the molecular dynamics simulations. Therefore, this compound was deemed to be potent as PPAR agonists.

Keywords:

PPAR agonist, Flavonoids, 3D-Pharmacophore, Molecular docking, Molecular dynamics simulation

1. INTRODUCTION

Metabolic syndrome (MetS) is a public health concern. A person is diagnosed with metabolic syndrome if they have three or more of the following symptoms: obesity, high blood pressure, and high blood triglyceride¹. MetS prevalence is affected by both non-modifiable genetic (gender, age, ethnicity) and modifiable (lifestyle, diet)² risk factors. Furthermore, the prevalence of MetS in children and youth has grown significantly within the last 10 years³⁻⁴. MetS affects approximately 20-25% of adults population⁵⁻⁶ and 19.2% of children⁷⁻⁸, with the risk being elevated among patients with type 2 diabetes⁹⁻¹⁰. MetS is a major cause of diabetics, coronary heart disease, and stroke⁸.

PPARs are a group of nuclear receptor proteins that induce ligand-dependent transcription of target genes, playing important roles in regulating metabolic activities⁹. The PPARs consist of three subtypes: PPAR α , PPAR β/δ ,

and PPAR γ ⁹. Currently, some PPAR agonists which act upon the PPARs are effectively used in the treatment of symptoms of MetS, such as fibrates (PPAR α agonists) for treating hypertriglyceridemia¹⁰, thiazolidinediones (PPAR γ agonists)¹¹ for slowing the progression of metabolic syndrome-related disorders, and PPAR δ agonists for increasing fatty acid oxidation¹². However, there are some adverse effects listed as weight gain, renal effects, congestive heart failure, fluid retention, myopathy and rhabdomyolysis.

Recently, there have been intensively researches to develop multitarget-directed PPAR agonists with the synergistic reaction as well as fewer side-effect in MetS¹³⁻¹⁸. For example, bezafibrate operated as a full agonist for all three PPAR isoforms¹³. Lanifibranor is a well-balanced pan-PPAR agonist¹⁴. Furthermore, many studies on flavonoids for activating PPARs, such as: formononetin could activate PPARs (EC₅₀=1.1 M)¹⁹, luteolin increased insulin sensitivity through PPAR activation²⁰, hesperidin

*Corresponding author:

*Phuong Thuy Viet Nguyen Email: ntvphuong@ump.edu.vn



Pharmaceutical Sciences Asia © 2023 by

Faculty of Pharmacy, Mahidol University, Thailand is licensed under CC BY-NC-ND 4.0. To view a copy of this license, visit <https://www.creativecommons.org/licenses/by-nc-nd/4.0/>

improved PPARs expression in the liver, adipocytes, therefore enhanced PPARs expression²¹. As a result, flavonoids are potential class of substances to develop drugs towards targeting PPARs.

In this study, the main goal was to discover flavonoid compounds as a potential agonist on three PPAR receptors. Initially, a 3D-pharmacophore model for the PPAR activators was constructed. Subsequently, flavonoids were screened through this model. Finally, molecular docking and molecular dynamics simulations were combined to select the potential substances for PPARs.

2. MATERIALS AND METHODS

2.1. 3D-pharmacophore modeling

The development process of 3D-pharmacophore model for PPAR activators was carried out by using MOE 2022.02 software²². Dataset included both training set and test set compounds. The training set (Table 1) consisted of 10 compounds with different structural backbones collected from the previous articles^{19,23-27}

(their EC₅₀ values for PPARs ranging from 0.29-9.55 μ M). The values were compared to the EC₅₀ value of bezafibrate on PPARs (EC₅₀=1.1 μ M). Bezafibrate is an agonist on all three PPARs. The test set had two groups, the active and non-active groups. 36 compounds belonged to the active group with their values of EC₅₀≤30 μ M. The non-active group included 18 inactive compounds (the EC₅₀ values>30 μ M)²⁰ and 288 decoys obtained from ZINC15 database through using Decoy Finder 2.0.

Energy minimization for all conformations of the compounds was conducted by using the Conformation Import tool. Pharmacophore Elucidation tool was used for generation of a 3D-pharmacophore model, and the Pharmacophore Search for Criteria was for assessment process. Criteria of evaluating pharmacophore model were the values of accuracy, overlap, sensitivity (Se), and specificity (Sp). If a greater number of active substances satisfy the model, the model's reliability increases, and vice-versa.

Virtual screening was then conducted through using a generated pharmacophore model. Library compounds for screening included 3,848 flavonoids obtained from

Table 1. PPAR agonists belong to the training set.

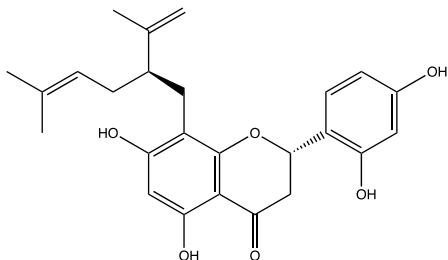
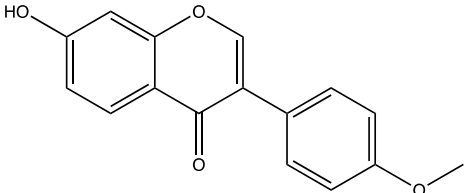
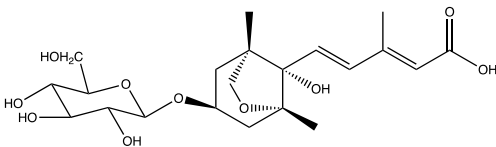
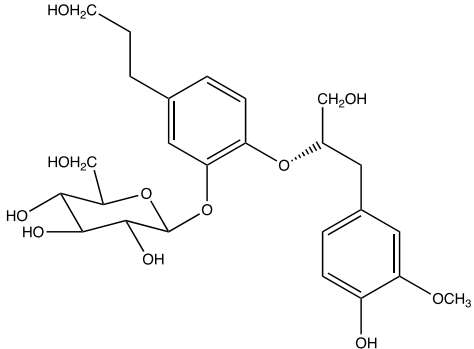
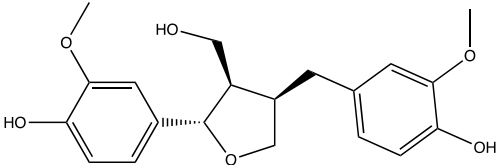
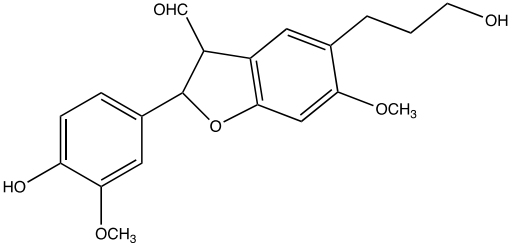
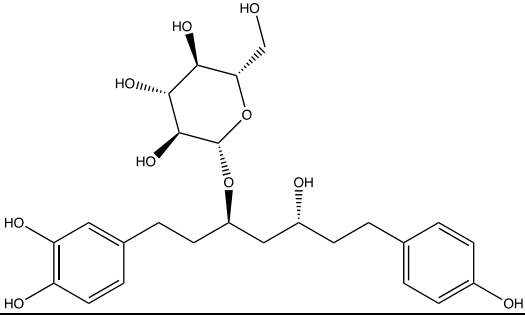
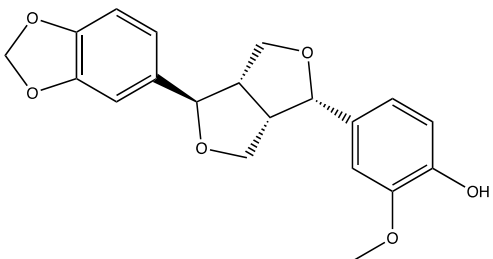
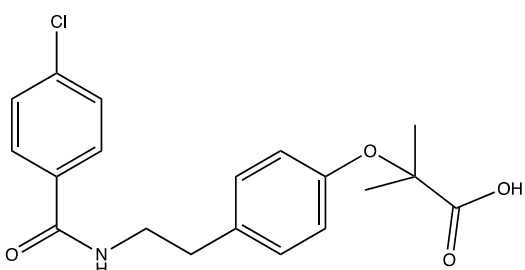
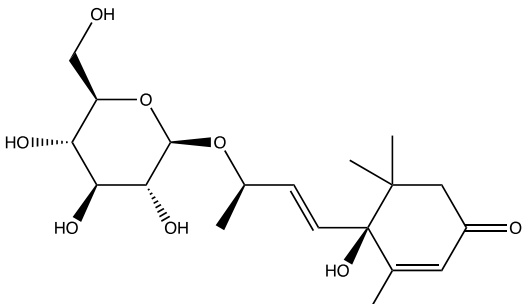
Name	Structure	EC ₅₀ values (μ M)	References
Norkurarinone		7.30	19
Formononetin		1.10	19
(2E,4E,1'R,3'S,5'R,8'S)-Dihydrophaseic acid 3'-O- β -D-glucopyranoside		9.55	23
(8S)-3-Methoxy-8,4'-oxyneolignan-4,9,9'-triol 3'-O- β -D-glucopyranoside		0.64	23

Table 1. PPAR agonists belong to the training set. (cont.)

Name	Structure	EC ₅₀ values (μM)	References
(+)-lariciresinol		1.47	23
5-(4-hydroxy-3-methoxyphenyl)-5-(3-hydroxypropyl)-6-methoxy-2-(3'-methoxy-4'-hydroxyphenyl)-3-benzofurancarboxaldehyde		4.32	23
3-O-β-D-glucopyranoside		0.29	25
Pluviatilol		1.64	26
		1.64	
Roseoside		1.55	27

PubChem database (<https://pubchem.ncbi.nlm.nih.gov/>). Compounds that satisfied the chemical features of the pharmacophore model were selected for further molecular docking.

2.2. Molecular docking

Three crystal structures of the PPARs: PPAR α (PDB: 5HYK), PPAR γ (PDB: 3NOA) and PPAR δ (PDB:

3GZ9) were downloaded from RCSB Protein Data Bank (<http://www.rcsb.org>). Re-docking of co-crystallized ligands into the main binding site of PPARs to evaluate the docking protocol. Subsequently, flavonoids satisfy chemical features of the model were docked into the PPARs after energy minimizing by using Chem3D 20.0 and converting to *.pdb format and saving as *.pdbqt. The docking program was AutoDock Vina 1.1.2²⁸ and docking parameters were listed in Table 2.

Table 2. Parameters of grid boxes for molecular docking of PPARs.

	PPAR α	PPAR γ	PPAR δ
Size x (Å)	26	26	26
Size y (Å)	26	26	26
Size z (Å)	26	26	28
Center x	10.186	-8.613	35.441
Center y	28.669	4.310	72.417
Center z	23.837	40.629	-0.793

2.3. Molecular dynamic simulations (MDs)

The potential candidate obtained from docking were subjected to MDs. The molecular dynamics simulations were run for both the complex of potential ligand and proteins and the apo proteins for 20 ns using Gromacs 2020.2 software²⁹. MDs investigated the stability and the flexibility of proteins and ligands and the protein-ligand complexes. The process included many stages: preparation of the topology, generation of a cubic simulation box and solvation in water, adding ions, energy minimization, system equilibration with a temperature of 300 °K and a pressure of 1 bar for 100 ps and running MDs. Viewing trajectories and analysing the results in terms of the values of RMSD (root-mean-square-deviation), RMSF (root-mean-square-fluctuation), hydrogen bond occupancy, Rg (radius of gyration) and solvent-accessible-surface area (SASA).

3. RESULTS AND DISCUSSION

3.1. 3D-pharmacophore modeling

Pharmacophore modeling was constructed based on different structural compounds with the PPAR activation EC₅₀ values. There are 17/83 (about 20%) pharmacophore models with an accuracy of 1.000³⁰. All 17 models are four-point pharmacophore models with good overlap scores (4.5575 to 6.1352). These models possessed at least one hydrophobic group and one hydrogen bond donor. It was compatible with the full agonist of PPARs, like the natural agent, eicosacoic³¹ acid and the synthetic compound, bezafibrate³² owning one hydrophobic domain and the other activating domain forming hydrogen bonds with key residues in the binding site of PPARs³³⁻³⁵.

The generated pharmacophore models consisted of four common pharmacophoric features, including one hydrophobic, two hydrogen acceptor, and one hydrogen

donor groups (Figure 1). Among 17 models, the pharmacophore model was chosen based on the values of high specificity (74%), high accuracy (74%), and high sensitivity (75%).

The pharmacophore model was used for the screening process of 3,848 flavonoids. The results revealed 648 flavonoids satisfying four chemical features of the model. Figure 2 illustrated these pharmacophoric features shared by flavonoids, i.e. the benzene ring of basic flavonoid skeletons as hydrophobic, hydroxyl group (-OH) or glucosyl substituents as a hydrogen bond donor, a methoxyl group (-OCH₃), carbonyl (-CO), and oxygen atom on the heterocycle as a hydrogen bond acceptor.

3.2. Molecular docking

Before performing molecular docking to explore binding modes of flavonoids with the PPARs, re-docking of the co-crystallized ligands into the main binding site of PPARs was conducted. The results revealed that the native ligands fitted well into the binding sites of PPARs with good docking scores: PPAR α (-11.6 kcal.mol⁻¹), PPAR γ (-11.5 kcal.mol⁻¹), PPAR δ (-12.2 kcal.mol⁻¹). The native ligands also had similar interactions with the re-docked ligands of PPARs and the root mean square deviation (RMSD) values obtained between them were 0.9345, 0.5044, 0.5336 (Å), respectively (Figure 3). These results confirmed the docking program's reliability, allowing to apply docking protocol for docking other ligands to explore the binding interactions of flavonoids and PPAR receptors.

In order to better understand the interactions of PPARs and flavonoids, molecular docking analysis was used. 648 flavonoids satisfying four chemical features of the model were explored to bind well into the PPARs with the binding affinities ranging from -5.6 to -11.0 kcal.mol⁻¹ (PPAR α), -6.9 to -10.9 kcal.mol⁻¹ (PPAR γ), -5.6 to -11.0 kcal.mol⁻¹ (PPAR δ). Analysis of binding

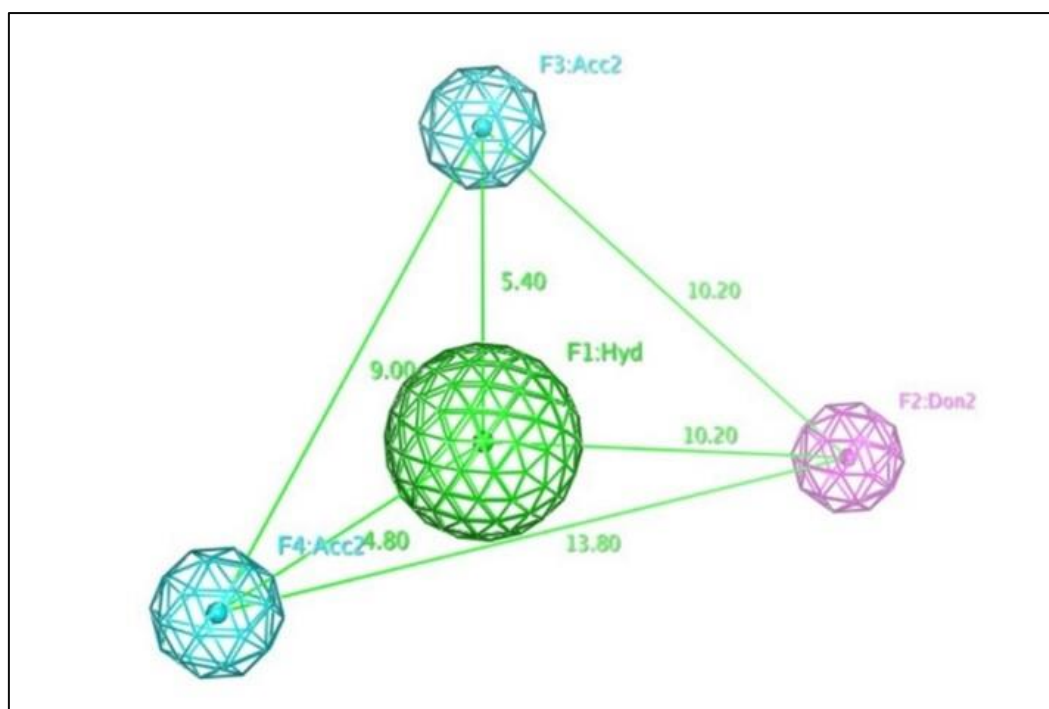


Figure 1. The pharmacophore model for PPAR activators with 4 points, including one hydrophobic (Hyd: green color), two hydrogen acceptors (Acc2: blue color), and one hydrogen donor (Don2: purple color).

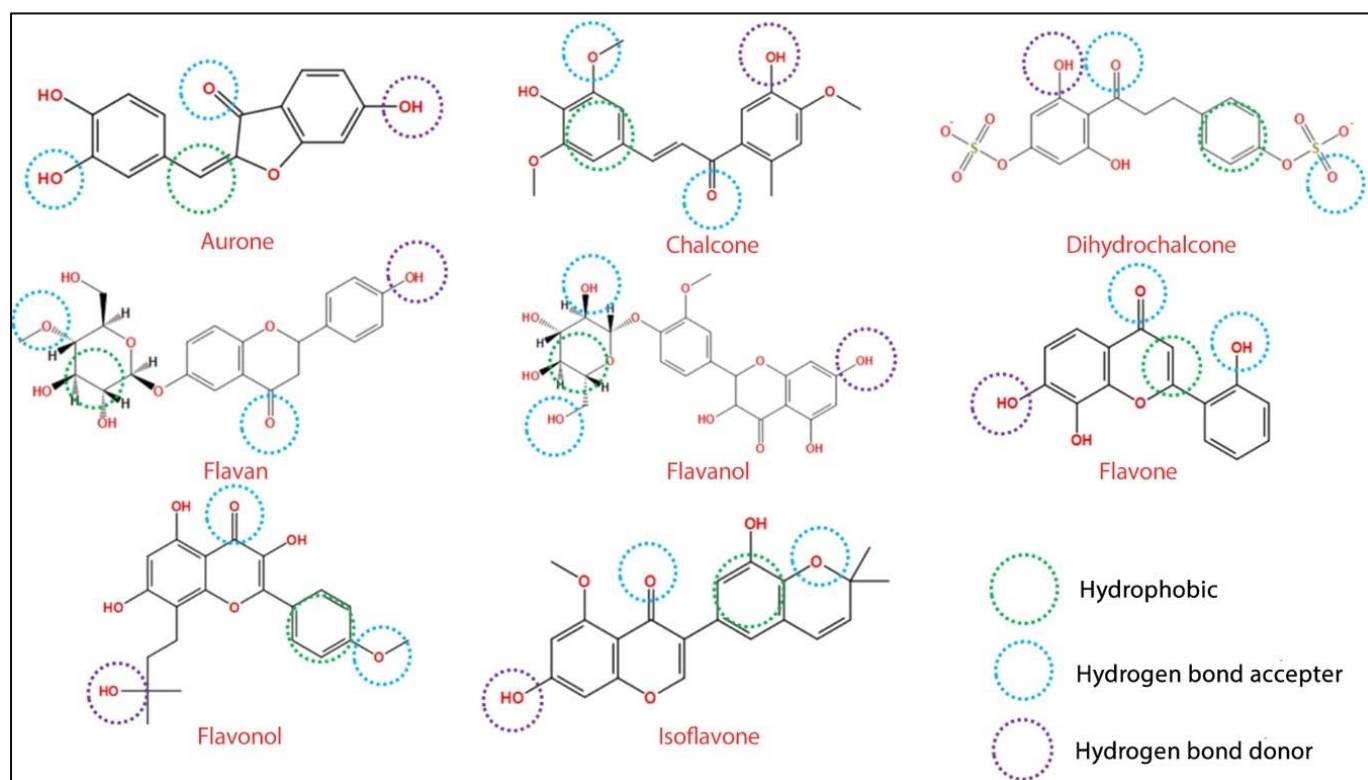
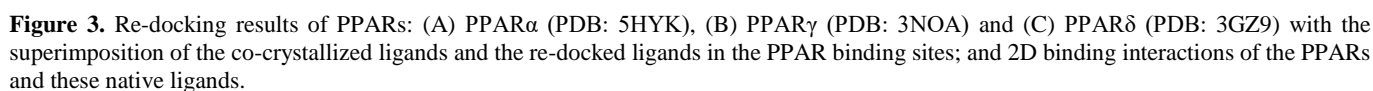


Figure 2. Illustration of four-point pharmacophoric features for PPARs shared by flavonoids compounds including aurone, chalcone, dihydrochalcone, flavan, flavanol, flavone, flavonol and isoflavone.



Our docking study suggested that F85 (5-Hydroxy-7-[3-O-(3,4,5-trihydroxybenzoyl)-beta-D-glucopyranosyloxy] flavone (Figure 4) was the most potential compound with the binding affinities into the PPAR α (-9.6

kcal.mol⁻¹), PPAR γ (-10.5 kcal.mol⁻¹) and PPAR δ (-9.5 kcal.mol⁻¹). The phenyl group of F85 was located in the arm of the one branch of the PPAR binding pocket, interacting with -OH of Tyr464 (PPAR α) or His449 and Tyr473 (PPAR γ) by hydrogen bonds. On the other hand, F85 aromatic rings also formed the hydrophobic interactions with Ile281, Gly284 towards the other branch of PPAR γ binding site. The Y-shaped cavity of PPAR δ is smaller than the ligand binding site of PPAR α and PPAR γ ³¹. Thus, it can be seen that F85 with bulky struc-

ture could not enter deeply in this binding site. However, this compound created other hydrogen bonds with the amine (NH_2 -) of Thr288, Thr289; ($-\text{CO}$) of Ile364 as well as hydrophobic interactions with His449, Val341, Leu33, Thr288 which helped to achieve good binding affinity with the receptor.

With PPAR α , flavonoids from the chalcone group owning bulky substituents such as glucosyl in F131, benzyl group in F465 were able to form hydrogen bonds with hydroxyl group of Tyr464 as well as one hydrophobic interaction with carbon chain of Leu321 involved in the binding cavity of PPAR α . Moreover, the key residue,

Tyr464 could also created hydrogen bonds with small substituents of flavonoids, such as hydroxyl group ($-\text{OH}$) in F95, F44, F93 and F96 (Figure 5).

In PPAR γ , most chalcone and dihydrochalcone interacted specifically with Cys285 of helix 3 through hydrophobic interaction. Figure 6 illustrated 5 flavonoids belonged to chalcone group with good binding affinities (-7.6 to -10.7 kcal.mol $^{-1}$). Hydroxyl group of A-ring of F99, glucosyl group of F484 and carbonyl group on A-ring of F73 formed a hydrogen bond with the side chain hydroxyl group of Tyr473.

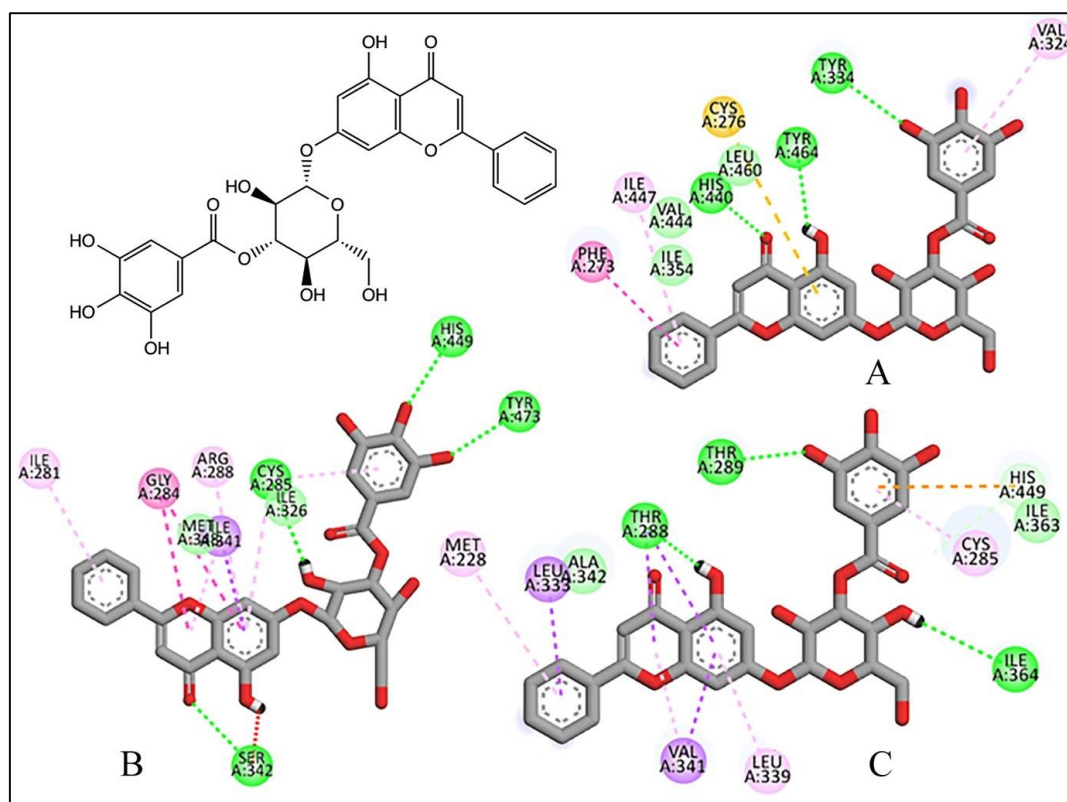


Figure 4. Structure of F85 and 2D binding interactions with green line represented for hydrogen bond; purple, pink, and yellow line for hydrophobic contacts after docking to PPARs (A: PPAR α , B: PPAR γ , C: PPAR δ).

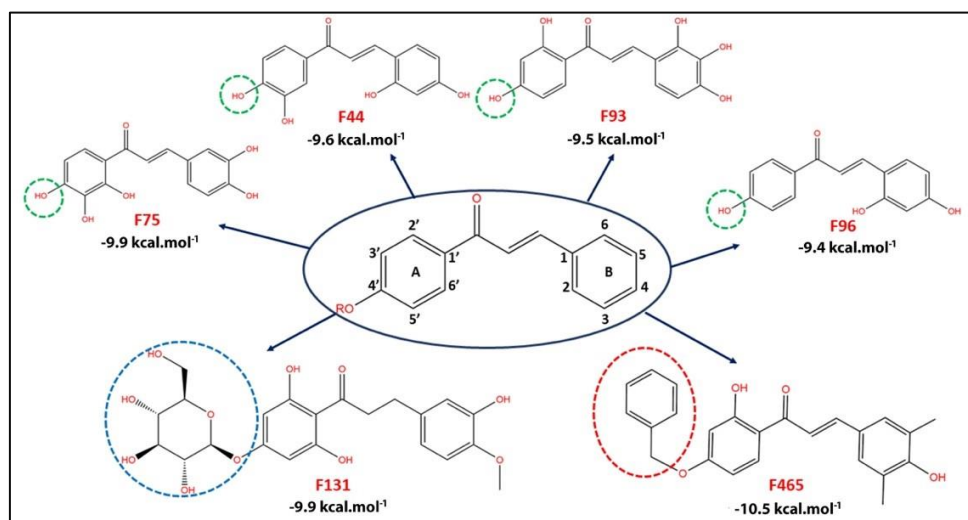


Figure 5. Illustration of flavonoids from the chalcone group with good binding affinities in the PPAR α (PDB: 5HYK).

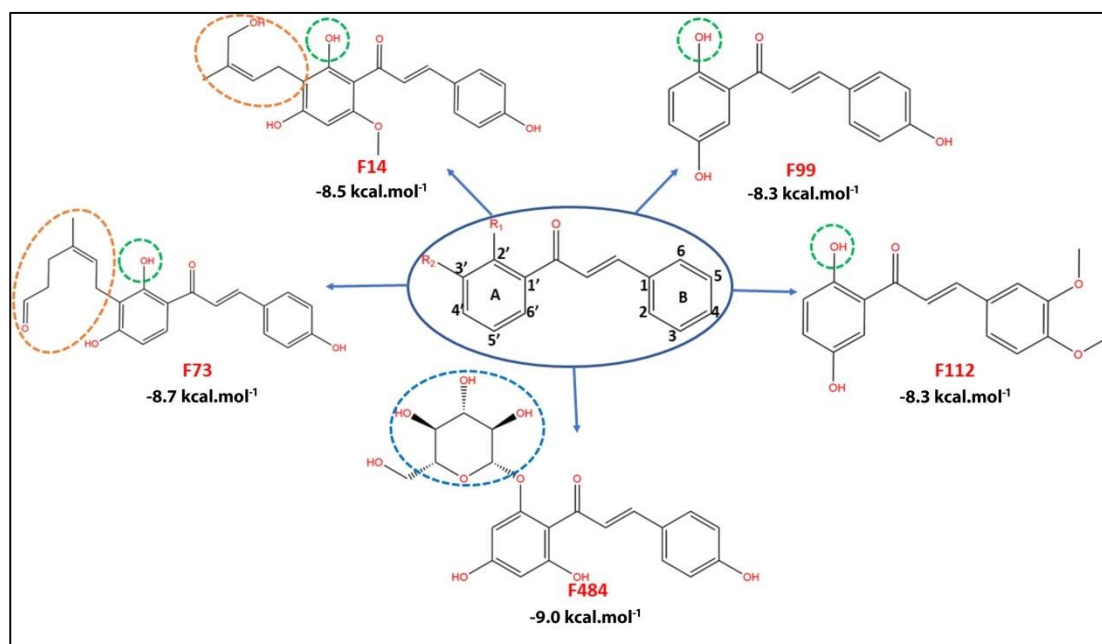


Figure 6. Illustration of flavonoids from the chalcone group with good binding affinity for PPAR γ (PDB: 3NOA).

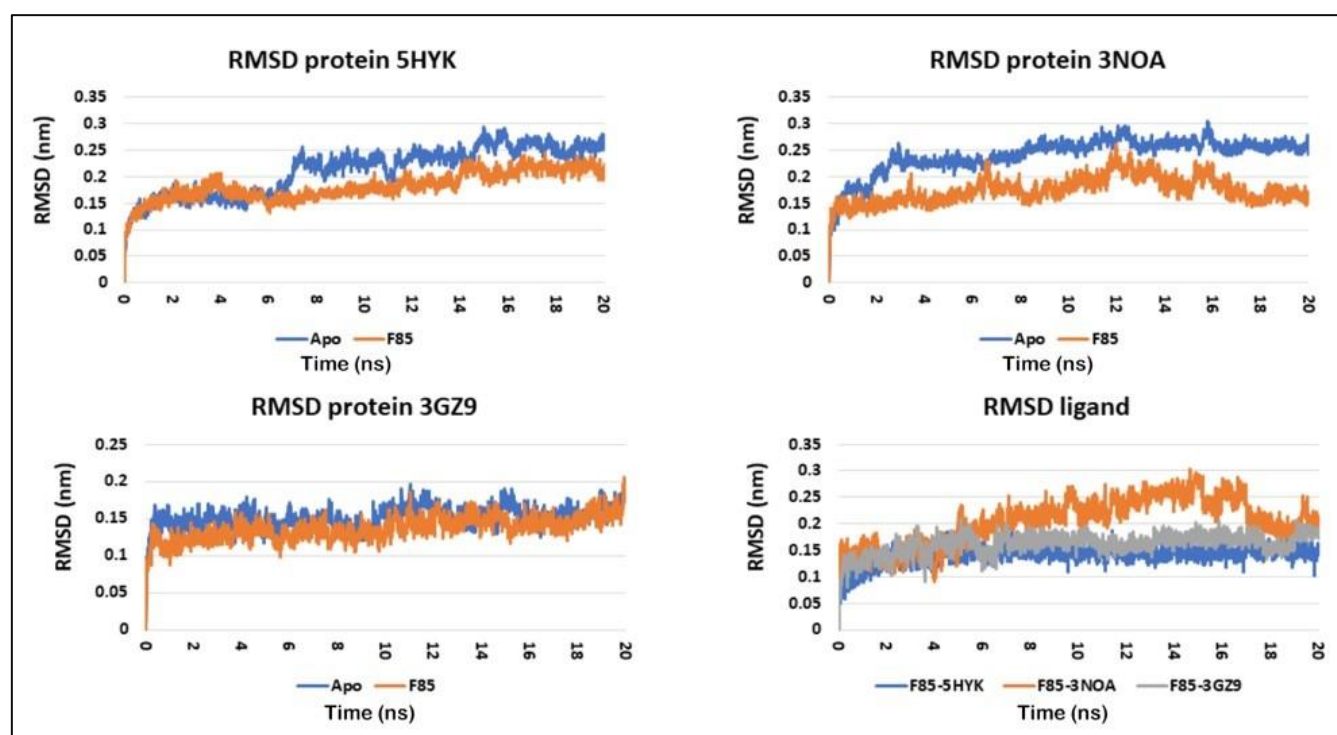


Figure 7. RMSD values of apo-proteins (PPAR α , PPAR γ , PPAR δ) compared to F85-PPARs complexes and RMSD of ligand F85 during 20 ns MDs.

3.3. Molecular dynamics simulations (MDs)

It was considered to be an efficient method for validating the stability of the predicted docked F85-PPARs complexes, 20 ns MDs studies of these complexes were performed. The MDs were analyzed by the values of RMSD (Figure 7), RMSF (Figure 8), Rg (Figure 9) and SASA (Figure 10) for the complexes and apo-proteins, showing that F85 was stable within the binding cavity of PPARs during 20 ns.

The complexes of F85-PPARs reached in a steady state at the early phase of the simulation. This study found that the RMSD of F85 complexes with PPAR α , PPAR γ , and PPAR δ were 0.1 nm, 0.2 nm, and 0.1 nm, respectively (Figure 7). The fluctuations remained within the range of 0.2 nm or 2.0 Å, indicating stabilization in the protein complex structure. The key amino acids in the binding site belonging to helices H3, H4, H5, H10, H11, and H12 showed lower RMSF values in the F85-PPARs complexes than apo-proteins. The histograms also showed

the Rg values were stable around 2 nm during 20 ns (Figure 9). Furthermore, there were no significant change in terms of SASA values during F85 binding to PPARs (Figure 10). That means PPARs remained steady state. For most of the simulations, F85 formed hydrogen bonds with all three PPARs with relatively high occupancy from 50 to 86% as follows: 6 hydrogen bonds formed between F85 and the PPAR α amino acids Phe273, Cys276, Thr289, Ser280, Ile317, Tyr334 and His440; 2 hydrogen bonds formed between F85 and the PPAR γ amino acids Ser342 and Arg288; and 3 hydrogen bonds formed between F85 and the PPAR δ amino acids Ala342, Lys367 and His449 (Figure 11).

Overall, it was shown that F85 binding tightly and stably into the binding sites of the three PPAR receptors. F85 formed the hydrogen bonds with key amino acids of PPARs and created hydrophobic interactions. The docking and MDs results were consistent. Of which, F85 maintained some hydrogen bonds with high occupancies such as Tyr334 (79.56%) and His440 (76.32%). However, some hydrogen bonds were unstable and replaced by hydrophobic interactions after running MDs. For example, with PPAR α , F85 interacted through hydrogen bonds with Tyr464, Tyr334, His440 as well as hydrophobic interaction with Cys276. However, the hydrophobic interaction with Cys276 changed into hydrogen bond with high occupancy (82.65%) and hydrogen bond with Tyr464 lost after running MDs, showing unstable of these interactions. With PPAR γ , after MDs, the interactions of F85 with the

receptor such as hydrogen bonds with His449, Tyr473; and hydrophobic interactions with Ile281, Gly284 were replaced by other hydrogen bonds with Ser342 and Arg288. It also happened with the complex of F85 and PPAR δ , the hydrogen bonds with Thr288, Thr289, Ile364 and hydrophobic interactions with His449, Val341, Leu333, Thr288 were lost. Only hydrogen bond between F85 and Thr289 existed with low occupancy (34.97%) and hydrophobic interaction with His449 was changed into hydrogen bonds (good occupancy of 82.74%).

Currently, there is no available study of F85 bio-activity. F85 is lipophilic with the value of logP of 1.26; and moderately soluble in water. This compound is a large natural compound with a bulky glucosyl group connected to phenyl, so F85 does not satisfy the Lipinski's rule of five. Thus, it was suggested for structural modification to design a full agonist on the PPARs.

Therefore, dual-agonist/pan-agonist activities on PPARs have the beneficial synergistic effect on Mets¹⁷. Clinical trials have shown that dual agonists can be safe and effective depending on the individual patient's condition³⁶. On the other hand, flavonoids are the potential compounds for research. They are also known as a potential class of substances to develop drugs towards targeting the PPARs. In line with the general trend of previous reports, this study has accomplished in the discovery of flavonoid compounds with high affinity of binding into all three PPARs, that are potentially activated by F85 compound.

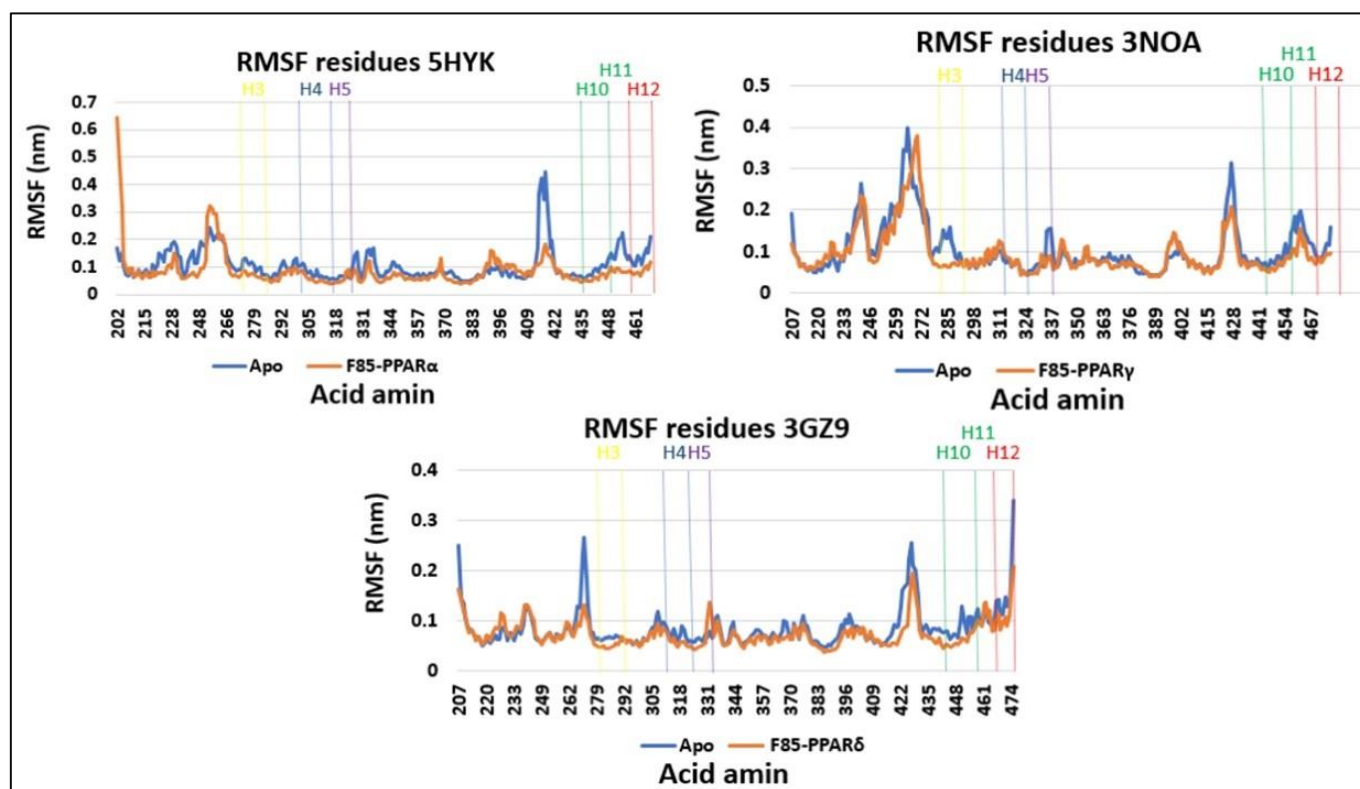


Figure 8. RMSF values of apo-proteins (PPAR α , PPAR γ , PPAR δ) compared to F85-PPARs complexes during 20 ns MDs.

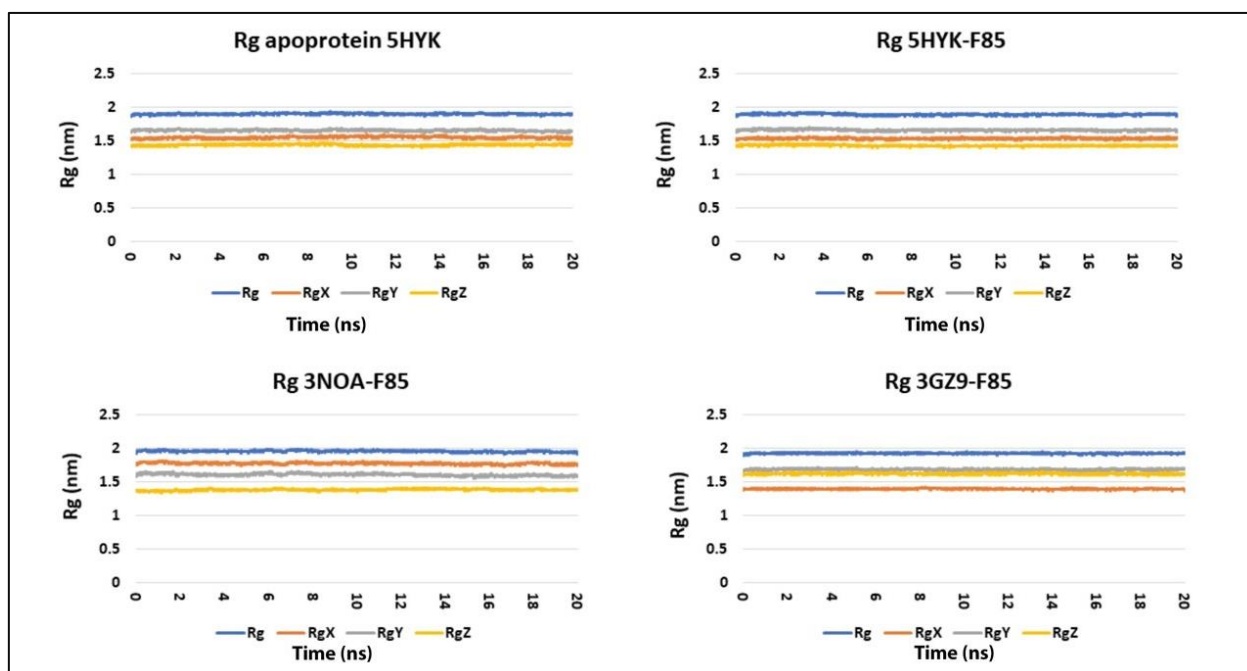


Figure 9. Rg values of apo-proteins (PPAR α , PPAR γ , PPAR δ) compared to F85-PPARs complexes during 20 ns MDs.

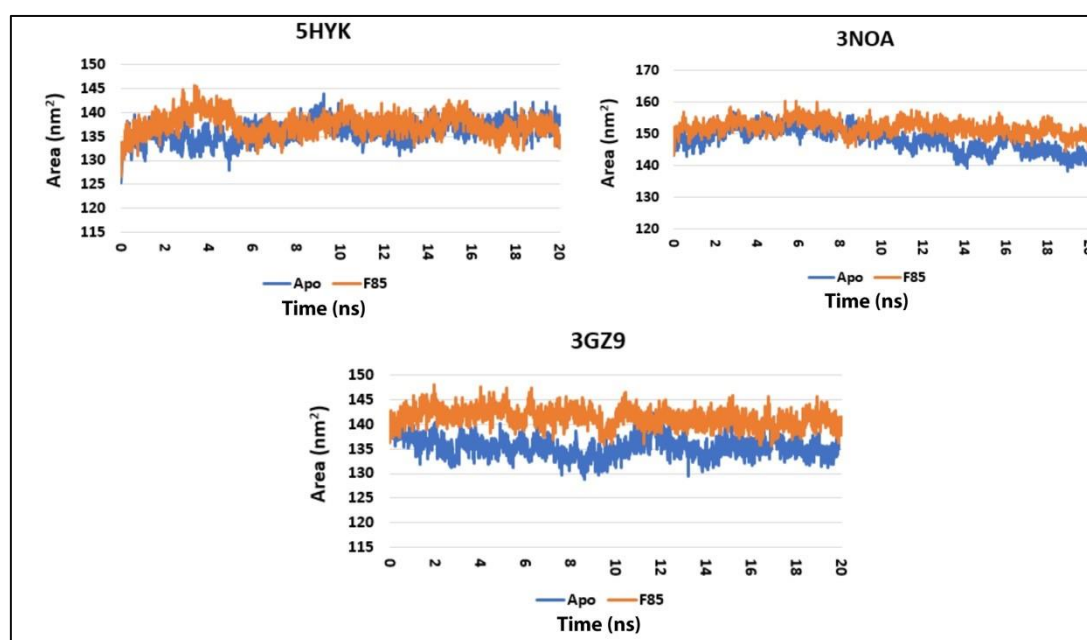


Figure 10. SASA values of apo-proteins (PPAR α , PPAR γ , PPAR δ) compared to F85-PPARs complexes during 20 ns MDs.

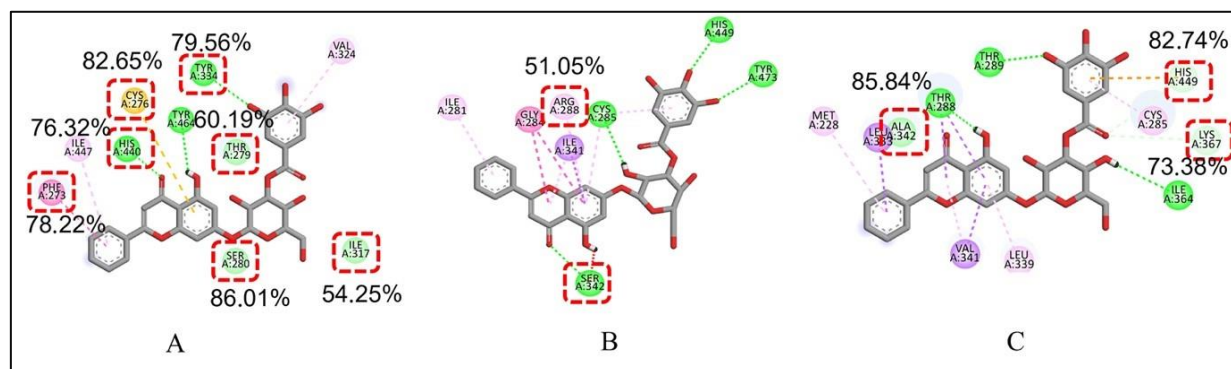


Figure 11. Percentage of hydrogen bonds between F85 and the residues of (A) PPAR α (PDB: 5HYK), (B) PPAR γ (PDB: 3NOA), (C) PPAR δ (PDB: 3GZ9) during 20 ns MDs.

4. CONCLUSION

In this study, an integrated three-step protocol including ligand-based pharmacophore modeling, molecular docking and molecular dynamics simulations was applied for virtual screening of the flavonoids database to discover novel PPAR agonists. 3,848 flavonoids were filtered through the constructed 3D pharmacophore model, with 648 compounds satisfied for chemical features. Based on molecular docking and MD simulations results, F85 showed the best binding affinity with the PPARs. F85 was stable in the three complexes with PPARs by forming the hydrogen bonds with key residues. These results revealed that F85 could be considered as a novel potential PPAR agonist. Further experimental studies, such as determining the binding capacity of F85 in PPARs, investigation of potential activating bioactivity of flavonoids on PPARs, and structural modification were required to improve the drug-likeness of F85.

5. ACKNOWLEDGEMENT

We would like to thank the University of Medicine and Pharmacy at Ho Chi Minh City, Viet Nam for the funding for this research.

Conflict of interest

There is no conflict of interest.

Funding

Funding from University of Medicine and Pharmacy at Ho Chi Minh, City

Ethics approval

None to declare.

Article info:

Received November 1, 2022

Received in revised form February 21, 2023

Accepted March 8, 2023

Author contribution

BHGN: virtual screening

PCUN: molecular docking

KAN: pharmacophore model

PNP: molecular docking

PTVN: study design, manuscript editing

REFERENCES

- Huang PL. A comprehensive definition for metabolic syndrome. *Dis Model Mech.* 2009;2(5-6):231-7.
- Nurillokizi NS. Metabolic Syndrome: Methods of Prevention and Treatment. *Barqarorlik va yetakchi tadqiqotlar onlayn ilmiy jurnali.* 2021;1(6):475-82.
- DeBoer MD. Assessing and managing the metabolic syndrome in children and adolescents. *Nutrients.* 2019;11(8):1788.
- Reisinger C, Nkeh-Chungag BN, Fredriksen PM, Goswami N. The prevalence of pediatric metabolic syndrome-A critical look on the discrepancies between definitions and its clinical importance. *Int J Obes.* 2021;45(1):12-24.
- Ranasinghe P, Mathangasinghe Y, Jayawardena R, Hills A, Misra A. Prevalence and trends of metabolic syndrome among adults in the asia-pacific region: a systematic review. *BMC Public Health.* 2017;17(1):1-9.
- Friend A, Craig L, Turner S. The prevalence of metabolic syndrome in children: a systematic review of the literature. *Metab Syndr Relat Disord.* 2013;11(2):71-80.
- Tan MC, Ng OC, Wong TW, Joseph A, Chan YM, Hejar AR. Prevalence of metabolic syndrome in type 2 diabetic patients: a comparative study using WHO, NCEP ATP III, IDF and Harmonized definitions. *Health.* 2013;5(10):2013.
- Cankurtaran M, Halil M, Yavuz BB, Dagli N, Oyan B, Ariogul S. Prevalence and correlates of metabolic syndrome (MS) in older adults. *Arch Gerontol Geriatr.* 2006;42(1):35-45.
- Dubois V, Eeckhoutte J, Lefebvre P, Staels B. Distinct but complementary contributions of PPAR isotypes to energy homeostasis. *J Clin Invest.* 2017;127(4):1202-14.
- Ghonem NS, Assis DN, Boyer JL. Fibrates and cholestasis. *Hepatology.* 2015;62(2):635-43.
- Nanjan M, Mohammed M, Kumar BP, Chandrasekar M. Thiazolidinediones as antidiabetic agents: A critical review. *Bioorg Chem.* 2018;77:548-67.
- Holst D, Luquet S, Nogueira V, Kristiansen K, Leverve X, Grimaldi PA. Nutritional regulation and role of peroxisome proliferator-activated receptor δ in fatty acid catabolism in skeletal muscle. *Biochim Biophys Acta.* 2003;1633(1):43-50.
- Tenenbaum A, Fisman EZ. Balanced pan-PPAR activator bezafibrate in combination with statin: comprehensive lipids control and diabetes prevention? *Cardiovasc Diabetol.* 2012;11:140.
- Boyer-Diaz Z, Aristu-Zabalza P, Andrés-Rozas M, Robert C, Ortega-Ribera M, Fernández-Iglesias A, et al. Pan-PPAR agonist lanifibranor improves portal hypertension and hepatic fibrosis in experimental advanced chronic liver disease. *J Hepatol.* 2021;74(5):1188-99.
- Capelli D, Cerchia C, Montanari R, Loiodice F, Tortorella P, Laghezza A, et al. Structural basis for PPAR partial or full activation revealed by a novel ligand binding mode. *Sci Rep.* 2016; 6:34792.
- Dinda B, Dinda M, Roy A, Dinda S. Dietary plant flavonoids in prevention of obesity and diabetes. *Adv Protein Chem Struct Biol.* 2020;120:159-235.
- Lefere S, Puengel T, Hundertmark J, Penners C, Frank AK, Guillot A, et al. Differential effects of selective-and pan-PPAR agonists on experimental steatohepatitis and hepatic macrophages. *J Hepatol.* 2020;73(4):757-70.
- Zhang J, Liu X, Xie XB, Cheng XC, Wang RL. Multitargeted bioactive ligands for PPAR s discovered in the last decade. *Chem Biol Drug Des.* 2016;88(5):635-63.
- Quang TH, Ngan NTT, Minh CV, Kiem PV, Tai BH, Nhiem NX, et al. Anti-inflammatory and PPAR transactivational properties of flavonoids from the roots of *Sophora flavescens*. *Phytother Res.* 2013;27(9):1300-7.
- Ding L, Jin D, Chen X. Luteolin enhances insulin sensitivity via activation of PPAR γ transcriptional activity in adipocytes. *J Nutr Biochem.* 2010;21(10):941-7.
- Jung UJ, Lee MK, Park YB, Kang MA, Choi MS. Effect of citrus flavonoids on lipid metabolism and glucose-regulating enzyme mRNA levels in type-2 diabetic mice. *In J Biochem Cell Biol.* 2006;38(7):1134-45.
- Molecular Operating Environment (MOE). version 2022.02. 1010 Sherbooke St. West, Suite #910, Montreal, QC, Canada: Chemical Computing Group ULC. H3A 2R7, 2022.
- Ngan NT, Quang TH, Tai BH, Song SB, Lee D, Kim YH, et al. Anti-inflammatory and PPAR transactivational effects of components from the stem bark of *Ginkgo biloba*. *J Agric Food Chem.* 2012;60(11):2815-24.
- Thao NP, Luyen BT, Ngan NT, Dat LD, Cuong NX, Nam NH, et

- al. Peroxisome proliferator-activated receptor transactivational effects in HepG2 cells of cembranoids from the soft coral *Lobophytum crassum* Von Marenzeller. *Arch Pharm Res.* 2015;38(5): 769-75.
25. Quang TH, Ngan NT, Minh CV, Kiem PV, Yen PH, Tai BH, et al. Diarylheptanoid glycosides from *Tacca plantaginea* and their effects on NF- κ B activation and PPAR transcriptional activity. *Bioorg Med Chem Lett.* 2012;22(21):6681-7.
26. Quang TH, Ngan NT, Minh CV, Kiem PV, Tai BH, Thao NP, et al. Anti-inflammatory and PPAR transactivational effects of secondary metabolites from the roots of *Asarum sieboldii*. *Bioorg Med Chem Lett.* 2012;22(7):2527-33.
27. Quang TH, Ngan NT, Minh CV, Kiem PV, Yen PH, Tai BH, et al. Plantagiolides I and J, two new withanolide glucosides from *Tacca plantaginea* with nuclear factor- κ B inhibitory and peroxisome proliferator-activated receptor transactivational activities. *Chem Pharm Bull.* 2012;60(12):1494-501.
28. Trott O, Olson AJ. AutoDock Vina: improving the speed and accuracy of docking with a new scoring function, efficient optimization, and multithreading. *J Comput Chem.* 2010;31(2):455-61.
29. Van Der Spoel D, Lindahl E, Hess B, Groenhof G, Mark AE, Berendsen HJ. GROMACS: fast, flexible, and free. *J Comput Chem.* 2005;26(16):1701-18.
30. Braga RC, Andrade CH. Assessing the performance of 3D pharmacophore models in virtual screening: how good are they? *Curr Top Med Chem.* 2013;13(9):1127-38.
31. Xu HE, Lambert MH, Montana VG, Parks DJ, Blanchard SG, Brown PJ, et al. Molecular recognition of fatty acids by peroxisome proliferator-activated receptors. *Mol Cell.* 1999;3(3): 397-403.
32. Abu-El-Zahab HS, Abdel Aal WE, Awadallah R, Mikhail TM, Zakaria K. The correlation between serum total cholesterol and some trace elements in serum, liver and heart of rats fed high cholesterol diet. *Nahrung.* 1991;35(8):827-34.
33. Kamata S, Oyama T, Saito K, Honda A, Yamamoto Y, Suda K, et al. PPAR α ligand-binding domain structures with endogenous fatty acids and fibrates. *iScience.* 2020;23(11):101727.
34. Muñoz-Gutierrez C, Adasme-Carreño F, Fuentes E, Palomo I, Caballero J. Computational study of the binding orientation and affinity of PPAR γ agonists: Inclusion of ligand-induced fit by cross-docking. *RSC Adv.* 2016;6(69):64756-68.
35. Fyffe SA, Alphey MS, Buetow L, Smith TK, Ferguson MA, Sørensen MD, et al. Recombinant human PPAR- β/δ ligand-binding domain is locked in an activated conformation by endogenous fatty acids. *J Mol Biol.* 2006;356(4):1005-13.
36. Cheng HS, Tan WR, Low ZS, Marvalim C, Lee JYH, Tan NS. Exploration and development of PPAR modulators in health and disease: an update of clinical evidence. *Int J Mole Sci.* 2019;20(20):5055.